

PAPER

## Low temperature photoconductivity of few layer $p$ -type tungsten diselenide ( $\text{WSe}_2$ ) field-effect transistors (FETs)

To cite this article: Sujoy Ghosh *et al* 2018 *Nanotechnology* **29** 484002

View the [article online](#) for updates and enhancements.





**IOP | ebooks**<sup>TM</sup>

Bringing you innovative digital publishing with leading voices to create your essential collection of books in STEM research.

Start exploring the collection - download the first chapter of every title for free.

# Low temperature photoconductivity of few layer *p*-type tungsten diselenide (WSe<sub>2</sub>) field-effect transistors (FETs)

Sujoy Ghosh<sup>1</sup>, Milinda Wasala<sup>1</sup>, Nihar R Pradhan<sup>2,3,4</sup>, Daniel Rhodes<sup>2</sup>, Prasanna D Patil<sup>1</sup> , Michael Fralade<sup>1</sup>, Yan Xin<sup>2</sup>, Stephen A McGill<sup>2</sup> , Luis Balicas<sup>2</sup> and Saikat Talapatra<sup>1,4</sup>

<sup>1</sup>Department of Physics, Southern Illinois University, Carbondale, IL 62901, United States of America

<sup>2</sup>National High Magnetic Field Lab, Florida State University, Tallahassee, FL 32310, United States of America

<sup>3</sup>Department of Chemistry, Physics and Atmospheric Science, Jackson State University, Jackson, MS 39217, United States of America

E-mail: [saikat@siu.edu](mailto:saikat@siu.edu) and [nihar.r.pradhan@jsums.edu](mailto:nihar.r.pradhan@jsums.edu)

Received 21 June 2018, revised 20 August 2018

Accepted for publication 11 September 2018

Published 1 October 2018



CrossMark

## Abstract

We report on the low-temperature photoconductive properties of few layer *p*-type tungsten diselenide (WSe<sub>2</sub>) field-effect transistors (FETs) synthesized using the chemical vapor transport method. Photoconductivity measurements show that these FETs display room temperature photo-responsivities of  $\sim 7 \text{ mA W}^{-1}$  when illuminated with a laser of wavelength  $\lambda = 658 \text{ nm}$  with a power of 38 nW. The photo-responsivities of these FETs showed orders of magnitude improvement (up to  $\sim 1.1 \text{ AW}^{-1}$  with external quantum efficiencies reaching as high as  $\sim 188\%$ ) upon application of a gate voltage ( $V_G = -60 \text{ V}$ ). A temperature dependent ( $100 \text{ K} < T < 300 \text{ K}$ ) photoconductivity study reveals a weak temperature dependence of responsivity for these WSe<sub>2</sub> phototransistors. We demonstrate that it is possible to obtain stable photo-responsivities of  $\sim 0.76 \pm 0.2 \text{ AW}^{-1}$  (with applied  $V_G = -60 \text{ V}$ ), at low temperatures in these FETs. These findings indicate the possibility of developing WSe<sub>2</sub>-based FETs for highly robust, efficient, and swift photodetectors with a potential for optoelectronic applications over a broad range of temperatures.

Supplementary material for this article is available [online](#)

Keywords: 2D materials, low-temperature transport, transition metal dichalcogenide, WSe<sub>2</sub>, phototransistor, electronic transport, optoelectronic transport

(Some figures may appear in colour only in the online journal)

## 1. Introduction

The inherent optical band gap present in a variety of two-dimensional van der Waals layered materials can possibly lead to devices with multifunctional photonics based applications [1]. In particular, high performance FETs based on layered transition metal dichalcogenides (TMDs) such as molybdenum disulfide (MoS<sub>2</sub>), tungsten disulfide (WS<sub>2</sub>), etc are thought of as ideal candidates for photodetectors and hence can lead to applications

pertaining to low power opto-electronics [2, 3]. In that respect recent investigations on monolayer to few-layers WSe<sub>2</sub> and their hetero-structures have indicated that these materials can display a variety of fundamental and interesting physics which may lead to future novel optoelectronic device applications [3–12]. For example, high-quality in-plane hetero-junctions of WSe<sub>2</sub> with MoSe<sub>2</sub> is a possible step forward for realizing in-plane transistors and diodes [6, 7], similar to WSe<sub>2</sub>-MoS<sub>2</sub> hetero-junctions which were shown to form lateral *p-n* diodes and photodiodes [9]. As such, understanding light-matter interaction in WSe<sub>2</sub>-based

<sup>4</sup> Authors to whom any correspondence should be addressed.

materials can lead to the development of these materials for niche optoelectronic applications.

Most of the recently reported FETs fabricated from few-layered WSe<sub>2</sub> crystals shows *p*-type characteristics [10–15], which can be further tuned by using different metals for the source and drain contacts [16, 17]. For example, by using Ni and Pd respectively for source and drain contacts, one can extract holes and electrons from the same channel and therefore observe ambipolar behavior from few-layered WSe<sub>2</sub> FETs [17]. One can observe the same ambipolar characteristic by using ionic liquid as the gate dielectric as reported on WSe<sub>2</sub> FET [18]. It was also demonstrated that FETs based on such few-layered WSe<sub>2</sub> flakes exfoliated from crystals grown through a chemical vapor transport (CVT) technique can display room temperature hole-mobilities approaching those of hole-doped Silicon [14]. The band gap values of these layered TMDs semiconductors typically lie between 1–2 eV and therefore show promising optical properties under exposure to visible light [19]. This is one of the reasons why TMDs and their hetero-structures are tested for their photo-responsive properties. A previous study on a photo-transistor based on monolayer WSe<sub>2</sub> [11] found much higher photo-responsivity ( $\sim 10^5$  AW<sup>-1</sup>) for low illumination intensity (2 W m<sup>-2</sup>) with a very slow switching time of several seconds ( $\sim 5$  s), similar to monolayer MoS<sub>2</sub> [20]. However, recent measurements on few-layered WSe<sub>2</sub> flakes show that it is possible to obtain high photo-responsivity  $\sim 7$  AW<sup>-1</sup>, as well as very short switching times of  $\sim 10$   $\mu$ s at room temperature when illuminated with white light [13]. These above mentioned studies on the optical properties of phototransistors based on WSe<sub>2</sub> and other layered TMDs, looks extremely promising, however, most of these characterizations performed were limited to room temperature. It is well known that device properties, which includes these 2D semiconductor devices as well, drastically changes at low temperature due to effects such as; (i) decrease of thermionic emission, which reduces the charge tunneling through metal-semiconductor junctions, (ii) increase of contact resistance, (iii) variation of trap states as well as recombination centers etc. Therefore, in order to expand the applicability of these materials further, it is extremely important to understand the temperature dependence of their optoelectronic properties. Of particular interest, how these few-layered semiconductors respond to light as a function of temperature (specifically at low temperatures), could lead to a better understanding of their optoelectronic properties and to applications where low temperature photo-detection is needed. In this report, we present the photo-response of few-layered WSe<sub>2</sub> FETs fabricated on the Si/SiO<sub>2</sub> substrate as a function of temperature and applied gate voltage. We observed the photo-responsivities, *R*, of  $\sim 1.1$  AW<sup>-1</sup>, with external quantum efficiencies (EQE) as high as  $\sim 188\%$ , is achievable in these devices upon application of gate voltage,  $V_G = -60$  V at 277 K, when illuminated with laser of wavelength,  $\lambda = 658$  nm ( $E = 1.88$  eV) under a laser illumination intensity,  $P_{\text{eff}} = 38$  nW. Such high quantum efficiency ( $>100\%$ ) indicates the possibility of generation of multiple photo carriers and recirculating them over the lifetime of the photo-generated carriers which leads to internal gain mechanisms [21] in our devices. Detailed temperature dependent (100 K  $< T < 300$  K) photoconduction

measurements, reveals that WSe<sub>2</sub> FETs show stable photo-responsivities of  $\sim 0.76 \pm 0.2$  AW<sup>-1</sup> ( $V_G = -60$  V) over the range of the temperatures studied, despite the mobility of the devices decreases as we lower the temperature.

## 2. Methods

Single crystals of WSe<sub>2</sub> were grown through CVT technique in a high temperature two-zone furnace using iodine as the transport agent. The 99.9% pure W (Acros Organics) and 99.5% pure Se (Acros Organics) were used for the crystal growth. The mixture of W and Se were heated at 1000 °C in a clean quartz tube in high purity iodine (1.5 mg cm<sup>-3</sup>) environment as the transport agent. The mixture was slowly heated from room temperature to the desired temperature 950 °C and 820 °C for both source and growth zone respectively and the experiment ran for 10 days. Then the furnace temperature slowly cooled down to the room temperature. The resulted bulk crystal were washed with hexane and dried in vacuum to remove any residual iodine from the crystal. Prior to our measurements, these crystals were characterized through photoluminescence spectroscopy, Raman spectroscopy, electron diffraction (EDX) and transmission electron microscopy in order to confirm the quality of the as grown crystals, which confirms the composition and crystal phase of WSe<sub>2</sub> as 2H-phase (trigonal prismatic), as reported in our previous studies [14, 22]. Highly *p*-doped Si is used for applying the back gate voltage. A bulk WSe<sub>2</sub> single-crystal was mechanically exfoliated by the scotch tape technique and thinner layered flakes were transferred onto a clean 270 nm thick SiO<sub>2</sub> substrate. FETs were fabricated via electron beam lithography techniques, followed by electron beam evaporation of 3/90 nm thick Ti/Au layers and subsequent lift-off with acetone. After lift-off and cleaning in acetone, the samples were thermally annealed at 300 °C for 3 h in forming gas to remove PMMA residue from the top of the WSe<sub>2</sub> channel. The devices were then vacuum-annealed at 130 °C for 24 h at high vacuum pressure (10<sup>-7</sup> Torr). Vacuum annealing improves the electrical contacts between the semiconductor and the metallic contacts as previously reported [14, 23]. The electronic and optoelectronic measurements were performed in a closed cycle helium flow vacuum probe station (JANIS SH-4-1) with a quartz optical window. After mounting the devices onto the cold head stage, the vacuum chamber was evacuated for  $\sim 2$  h to reach the pressure of  $\sim 10^{-5}$  Torr. The 3-terminal FET measurements were performed by using Keithley 2400 series source meter units. For optoelectronic measurements a continuous wave laser light source (coherent cube,  $\lambda = 658$  nm) with tunable laser illumination intensity was mounted close to the optical window and separated from the cryostat body.

## 3. Results and discussions

Figure 1(a) displays the optical image of one of the WSe<sub>2</sub> FET on a Si/SiO<sub>2</sub> substrate. The dimensions of the sample, depicted in figure 1(a), are  $L/W \sim 9.0 \mu\text{m}/5.2 \mu\text{m}$ , where *L*

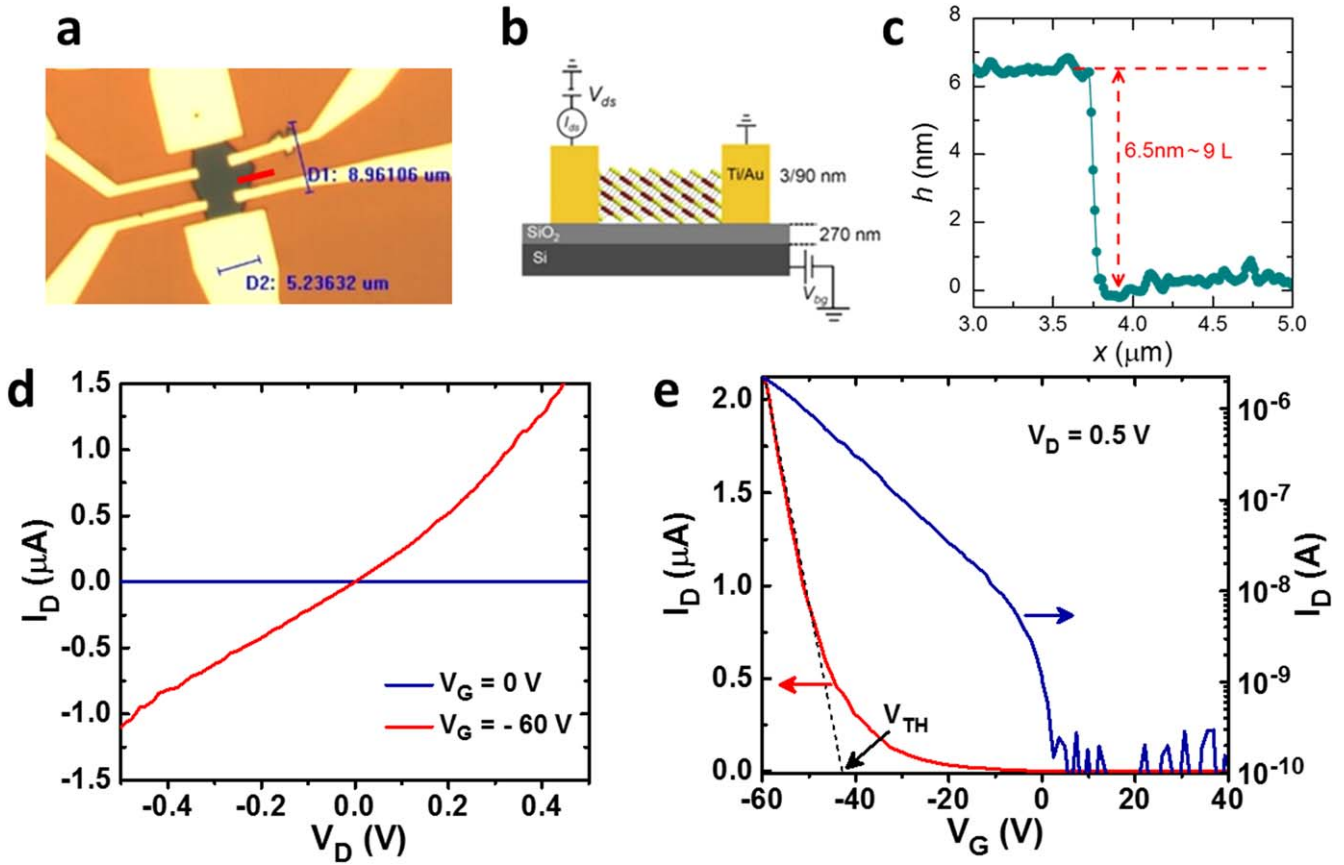


**Figure 1.** (a) Optical micrograph image of one of our fabricated WSe<sub>2</sub> field-effect transistors with Au on Ti for the electrical contacts. (b) Schematic of our FETs when measured in a three-terminal configuration. (c) AFM height profile measured across the edge of the WSe<sub>2</sub> channel indicating a 6.5 nm thick crystal, corresponding to nine atomic layers. (d) Drain to source current,  $I_D$ , as a function of bias voltage,  $V_D$  without the application of a gate voltage,  $V_G = 0$  V (blue markers) and under the application of a gate voltage  $V_G = -60$  V (red markers). (e) The field-effect electrical transport measurement under a constant source to drain voltage  $V_D = 0.5$  V and under varying  $V_G$  in normal scale (red marker) and in semi logarithmic scale (blue marker) in order to estimate the ON/OFF ratio of the device.

and  $W$ , are length and width of the channel, respectively. Figure 1(b) depicts the schematic of the FET and the scheme of measurements based on three-terminal configuration. Figure 1(c) displays the AFM height profile indicating that channel is composed of nine atomic layers.

Electrical transport characterization of one of our devices ( $\sim 277$  K) is shown in figures 1(d) and (e). Figure 1(d) shows the drain to source current ( $I_D$ ) as a function of the drain to source bias voltage ( $V_D$ ) under  $V_G = -60$  V (red marker) and also without the application of any gate voltage (blue marker). From the data it is clear that the application of a gate voltage substantially increases the channel current due to electrostatic doping. Notice that  $I_D$  as a function of  $V_D$  curve measured under voltage window of  $-0.5$  V  $< V_D < 0.5$  V indicates a linear region at the source to drain bias  $V_D < 0.2$  V and becomes nonlinear at  $V_D > 0.2$  V. Nonlinearity in the  $I_D$ - $V_D$  behavior is usually due to the Schottky barrier at junction between metallic contact and semiconductor channel, and is discussed in greater detail (specifically for WSe<sub>2</sub> FETs) in a previous article [14]. The field-effect electronic transport properties of the WSe<sub>2</sub> FET, measured with a 3-terminal back-gated configuration at room temperature and under  $V_G$ , ( $-60$  V  $< V_G < 40$  V) is shown in figure 1(e) (red marker)

under a constant  $V_D = 0.5$  V. The back-gated transfer characteristics ( $I_D$  as a function of  $V_G$  curve) shows typical  $p$ -type conduction, with a threshold gate voltage,  $V_{TH}$  of  $\sim -43$  V for this particular device. The current ON/OFF ratio was found to be  $\sim 10^4$  as shown in figure 1(e). From this measurement, the field-effect hole mobility ( $\mu_{FE}$ ) was calculated using the formula  $\mu_{FE} = (1/C_{ox}) \cdot (1/V_D) \cdot (L/W) \cdot (\partial I_D / \partial V_G)$ , where,  $C_{ox}$  is the capacitance per unit area of the 270 nm SiO<sub>2</sub>. The field-effect mobility for reported device was found to be  $\mu_{FE} \sim 80$  cm<sup>2</sup> V<sup>-1</sup> s<sup>-1</sup>. For a TMD-SiO<sub>2</sub> interface, typically the number density of interface trap states lies in the order of  $n_{trap} \sim 10^{11}$ - $10^{12}$  cm<sup>-2</sup> and for our devices typical trap density was  $n_{trap} \sim 3.36 \times 10^{11}$  cm<sup>-2</sup>. We have utilized the hysteresis behavior of the device upon gate sweep in order to estimate this number as shown in supplementary figure (S1 supplementary information is available online at [stacks.iop.org/NANO/29/484002/mmedia](https://stacks.iop.org/NANO/29/484002/mmedia)). Such generic  $p$ -type electrical behaviors were also seen on other devices as well, one of which (device II) is presented in figure S3 of the supplementary information.

Room temperature photodetection ability of WSe<sub>2</sub> FET is presented in figure 2. Photoconduction measurements were investigated using a red laser of wavelength  $\lambda = 658$  nm

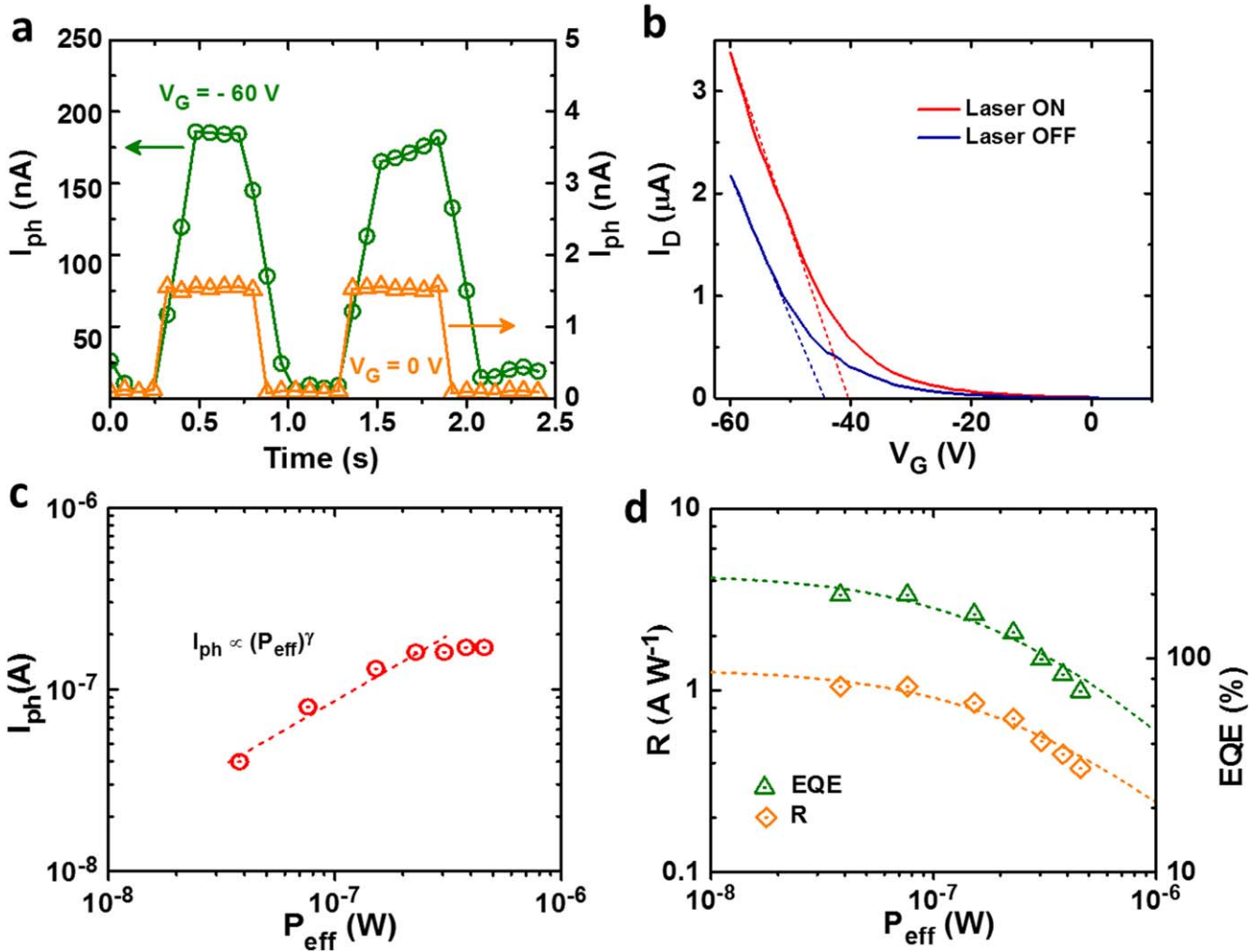


**Figure 2.** (a) Photocurrent response under laser ON and OFF cycling, measured without the application of a gate voltage (i.e.  $V_G = 0$  V, orange markers) and under the application of a gate voltage  $V_G = -60$  V (green markers) with  $V_D = 0.5$  V. (b) Transfer characteristics under no light illumination (laser OFF) and under illumination intensity of  $P_{\text{eff}} \sim 1.2 \mu\text{W}$  (laser ON). (c) Photocurrent,  $I_{\text{ph}}$ , as a function of illumination intensity,  $P_{\text{eff}}$ , under gate bias voltage,  $V_G = -60$  V. Dashed line shows power law behavior,  $I_{\text{ph}} \propto (P_{\text{eff}})^{\gamma}$ . (d) Responsivity,  $R$ , and external quantum efficiency, EQE, as a function of illumination intensity,  $P_{\text{eff}}$ , under gate bias voltage,  $V_G = -60$  V. Dashed lines are fit of form  $R = A_1/(A_2 + P_{\text{eff}})$  and  $\text{EQE} = B_1/(B_2 + P_{\text{eff}})$  as demonstrated by Roy *et al* [33] with  $A_1$ ,  $A_2$ ,  $B_1$  and  $B_2$  are fitting parameter.

( $E = 1.88$  eV) with a circular spot size of diameter  $\sim 3$  mm. Since the spot size is much larger than the actual device size, the effective intensity illuminating the device ( $P_{\text{eff}}$ ) was estimated by using the formula  $P_{\text{eff}} = (A_{\text{device}}/A_{\text{laser}}) P_{\text{total}}$ . Here, we would like to note that, larger spot size meant that under illumination both the source and the drain contacts were equally illuminated. Under these conditions the temperature gradient can be assumed to be negligible across the channel minimizing the photo-thermoelectric effect [24].

Figure 2(a) shows the photocurrent response of the device under cyclic laser ON and OFF conditions in absence and with the application of a gate voltage at  $T = 277$  K (with  $P_{\text{eff}} = 0.46 \mu\text{W}$  and  $V_D = 0.5$  V). The photocurrent  $I_{\text{ph}} = I_{\text{illu}} - I_{\text{dark}}$ , where  $I_{\text{illu}}$  is the current obtained under laser illumination and  $I_{\text{dark}}$  is the current obtained under dark conditions. At  $V_G = 0$  V,  $I_{\text{ph}}$  was found to be  $\sim 1.5$  nA. However, under  $V_G = -60$  V, our WSe<sub>2</sub> FET device showed  $I_{\text{ph}} \sim 200$  nA, which is two orders of magnitude higher than the value obtained without gate bias. This behavior is similar

to past investigations [12, 13, 15] where it was shown that the photocurrent, and hence the responsivity, increases orders of magnitude in the ON-state of WSe<sub>2</sub> phototransistor.

Figure 2(b) shows transfer characteristics with laser OFF and laser ON (under  $P_{\text{eff}} \sim 1.2 \mu\text{W}$ ). It was noted that on-state  $I_D$  increased from  $2.2 \mu\text{A}$  under the laser OFF condition to  $3.4 \mu\text{A}$  under laser ON condition at an applied  $V_G = -60$  V. Also a  $V_{\text{TH}}$  shift from  $-43$  to  $-40$  V upon laser illumination was observed. Such behavior is observed in a variety of 2D phototransistors [15, 20, 21, 24–26] and can be explained in the light of presence of several different mechanisms such as photoconductive as well as photogating [27, 28]. In the case of pure photoconduction, the photocurrent will be linearly dependent on incident photon flux or in other words, on illumination intensity i.e.  $I_{\text{ph}} \propto (P_{\text{eff}})^{\gamma}$ , where  $\gamma \sim 1$ . However in the presence of photogating effect,  $\gamma$  will deviate from 1, particularly  $\gamma < 1$  [24, 25]. Figure 2(c) shows  $I_{\text{ph}}$  as a function of  $P_{\text{eff}}$  under  $V_G = -60$  V. At low intensities, we found that the photocurrent follows a power



law behavior,  $I_{\text{ph}} \propto (P_{\text{eff}})^\gamma$  with  $\gamma = 0.56$ . We believe that in our WSe<sub>2</sub> devices, the sublinear dependence of the photocurrent ( $I_{\text{ph}} \sim P_{\text{eff}}^{0.5}$ ) in the ON-state clearly suggests that the dominant mechanism for the strong enhancement of the photocurrent upon application of gate is due to photogating effect. Further, in case of pure photoconduction, photo-generated electron–hole pair recombining through band to band transition whereas in case of photogating, photo-generated electron–hole pair recombining via charge traps at surface and interface. Time scale associated with band to band transition is usually faster than time scale associated with charge trapping and de-trapping. Thus, photo-response rise/fall time due to photogating effect is slower than those due to photoconductive effect. An analysis of the time response extracted from our data presented (device I) in supplementary figure S2 indicates that for an applied  $V_G = -60$  V, the estimated fall time is at least 3 times slower than the response of the device without the application of any gate voltage indicating the importance of charge trapping de-trapping due to photogating effect and could be the reason for the observed high gain in our devices as described below.

Typically, photo-responsivity ( $R$ ) and EQE are the two most critical quantities to be considered to evaluate the overall performance of a photo detector and they are defined as  $R = I_{\text{ph}}/P_{\text{eff}}$  and  $\text{EQE} = R (h.c/e.\lambda)$ , where  $h$  is the Plank's constant,  $\lambda$  is the excitation wavelength and  $e$  is the electron charge. For this device the maximum photo-responsivity at room temperature with  $V_G = 0$  V and  $P_{\text{eff}} = 38$  nW was found to be  $\sim 7$  mA W<sup>-1</sup>. Under  $V_G = -60$  V, both photo-responsivity and concomitant EQE values can be enhanced by two orders of magnitude than  $V_G = 0$  V. For example, for this device, photo-responsivity (with  $P_{\text{eff}} = 38$  nW and  $V_G = -60$  V) was found to be  $\sim 1.1$  A W<sup>-1</sup> with a corresponding EQE  $\sim 188\%$ . The dependence of the photo-responsivity and EQE on the illumination intensity at 277 K is shown in figure 2(d). These values are comparable and in some cases, better than those obtained for several other 2D photo-active crystals [28–30].

To check the performance of the WSe<sub>2</sub> phototransistors for potential applications in places where operating temperatures are substantially lower than ambient temperature, we have performed photocurrent measurements on these devices over a temperature range of  $100 \text{ K} < T < 277 \text{ K}$ . The temperature dependent transfer characteristics of the device is shown in figure 3(a). The device showed consistent  $p$ -type behavior over the entire range of temperatures studied. On-state  $I_D$  decreased from  $2.2 \mu\text{A}$  at 277 K to  $0.2 \mu\text{A}$  at 115 K. Field-effect hole mobility ( $\mu_{\text{FE}}$ ) also decreased from  $\sim 80 \text{ cm}^2 \text{ V}^{-1} \text{ s}^{-1}$  at 277 K to  $8 \text{ cm}^2 \text{ V}^{-1} \text{ s}^{-1}$  at 115 K, as shown in inset of figure 3(a). However, a substantial photocurrent was obtained over the entire range of studied temperatures. Transfer characteristics at  $T = 115$  K, as shown in figure 3(b), displays an increment in the ON-state  $I_D$  and shift in the threshold voltage under  $P_{\text{eff}} = 0.46 \mu\text{W}$ . Inset of figure 3(b) shows photo-response of the device under cyclic laser ON and OFF conditions with and without  $V_G$  at  $T = 115$  K, which exhibit an order of magnitude increment for  $V_G = -60$  V compared to  $V_G = 0$  V. Under  $V_G = -60$  V, our WSe<sub>2</sub> FET shows an increase in  $I_{\text{ph}}$  with increasing  $P_{\text{eff}}$  at  $T = 115$  K and it follows a power dependence,  $I_{\text{ph}} \propto (P_{\text{eff}})^\gamma$ , with  $\gamma = 0.5$ , as shown in

figure 3(c). The exponent,  $\gamma$  was found to be  $\sim 0.5$  for the range of temperatures studied and is shown in the inset of figure 3(c). We further found that the responsivity, as shown in figure 3(d), remains almost constant under a fixed  $P_{\text{eff}}$  and  $V_G$  over the temperature range  $115 \text{ K} < T < 277 \text{ K}$ .

A strong temperature dependence of the photocurrent has been observed in many disordered bulk semiconductors and more recently in CVD grown monolayer MoS<sub>2</sub> [31]. Such temperature dependences are generally attributed due to trapping and un-trapping of the photo-generated carriers by localized defect states, usually referred as trap states [31]. Since these trap states are themselves thermally activated, a strong temperature dependence of the photocurrent expected, specifically photocurrent becomes more prominent towards higher temperatures (photocurrent increases as temperature increases). Further, depending on the energy distribution of the of trap states, they can be classified as deep traps (located close to the mid-gap) and shallow trap states (located closer to the valence or conduction band edges). In the case of  $p$ -type WSe<sub>2</sub>, it has been recently reported by Kim *et al* [32] that the majority of trap states are located near the valence band edge (shallow trap states). In our WSe<sub>2</sub> phototransistors, we observe a very weak temperature dependence of photocurrent over the range of temperatures studied. A detail dependence of photo-responsivity ( $R$ ) of another device (device III), as function of gate voltage and drain voltage ( $V_D$ ) at constant effective intensity illuminating of  $P_{\text{eff}} = 605$  nW and constant temperature  $T = 275$  K is provided in supplementary information (figure S4(b)). Photo-responsivity as function of gate voltage and temperature ( $T$ ) at constant effective intensity illuminating of  $P_{\text{eff}} = 605$  nW and at drain voltage,  $V_D = 0.5$  V for this same device is shown in figure S4(c). We found that for this device photo-responsivity increased upon application of back gate voltage ( $V_G$ ) and/or upon application of drain voltage ( $V_D$ ). A weak dependence of the photo-responsivity under a fixed  $P_{\text{eff}}$  and  $V_G$  over the temperature range  $75 \text{ K} < T < 275 \text{ K}$  was also observed.

With several analysis presented, the low temperature photo-response seen in our samples may be attributed to the fact that, the majority of the trap states are shallow trap states and due to the lower activation energy of these states, they can participate in photocurrent generation at lower temperatures. This assertion can be further strengthened by the fact that the power exponent,  $\gamma$  remains close to 0.5 over the whole range of studied temperatures. These investigations show that few-layered CVT grown WSe<sub>2</sub> is a suitable candidate for developing high performance photodetectors with substantial temperature stability.

#### 4. Conclusions

In conclusion, we have shown that few layer  $p$ -type WSe<sub>2</sub> shows robust photo-responsive behavior over a wide range of temperatures. The similarities in the photo-conducting behavior of few layer  $p$ -type WSe<sub>2</sub> with other layered TMD materials, such as fractional power dependence of the photocurrent on the illumination intensity of the laser, enhancement of the responsivity with the application of a gate voltage, etc was observed.

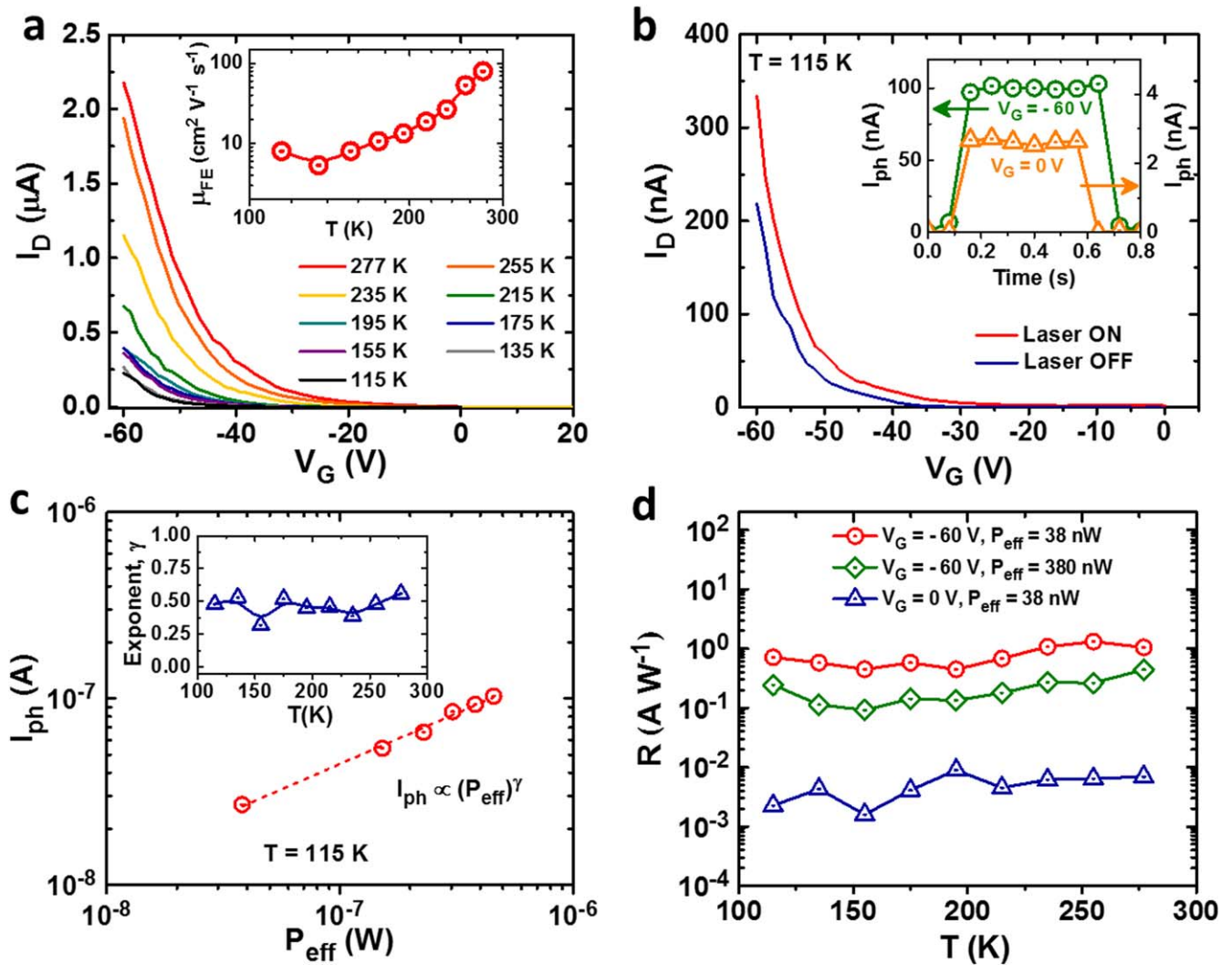


**Figure 3.** (a) The FET behavior of the device over a temperature range of  $115\text{ K} < T < 277\text{ K}$ . inset shows variation of mobility with temperature. (b) Transfer characteristics under no light illumination (laser OFF, blue marker) and under illumination intensity of  $P_{\text{eff}} = 0.46\ \mu\text{W}$  (laser ON, red marker) at  $T = 115\text{ K}$ . Inset shows photocurrent response under laser ON and OFF cycling, measured without the application of a gate voltage (i.e.  $V_G = 0\text{ V}$ , orange markers) and under the application of a gate voltage  $V_G = -60\text{ V}$  (green markers). (c) Photocurrent,  $I_{\text{ph}}$ , as a function of illumination intensity,  $P_{\text{eff}}$ , under gate bias voltage,  $V_G = -60\text{ V}$ . Dashed line shows power law behavior,  $I_{\text{ph}} \propto (P_{\text{eff}})^{\gamma}$ . Inset: variation of the exponent,  $\gamma$ , over a range of studied temperatures. (d) Responsivity,  $R$ , as a function of temperature at different illumination intensity,  $P_{\text{eff}}$ , and gate voltage,  $V_G$ .

However, this study also provided evidence for a substantially different temperature dependence with respect to the photo-responsivity reported so far on other TMD materials. In the present study, a very weak temperature dependence was observed for the photocurrent, and thus for the photo-responsivity, over a wide range of temperatures. We believe that the presence of shallow trap states in CVT grown  $\text{WSe}_2$  samples is perhaps one of the reasons for their photo-responsivities even at low temperatures. These measurements, to our knowledge, are the first measurements available on low temperature photoconductivity of  $p$ -type  $\text{WSe}_2$  FETs. As such these studies are extremely valuable for understanding the fundamental physical nature of photoconduction in these materials at low temperatures. These results also suggest that the photo-transistors based on  $\text{WSe}_2$  crystals might have advantages over other 2D crystals for low-temperature photodetection. These

findings indicate the possibility of developing  $\text{WSe}_2$ -based FETs as robust, efficient, and swift photodetectors with potential for optoelectronic applications operating over a wide range of temperature.

### Acknowledgments

This work was supported by the US Army Research Office MURI Grant W911NF-11-1-0362.

### ORCID iDs

Prasanna D Patil <https://orcid.org/0000-0002-9296-1102>  
Stephen A McGill <https://orcid.org/0000-0001-6365-7155>

## References

- [1] Xia F, Wang H, Xiao D, Dubey M and Ramasubramaniam A 2014 Two-dimensional material nanophotonics *Nat. Photon.* **8** 899–907
- [2] Li S-L, Tsukagoshi K, Orgiu E and Samori P 2016 Charge transport and mobility engineering in two-dimensional transition metal chalcogenide semiconductors *Chem. Soc. Rev.* **45** 118–51
- [3] Doganov R A *et al* 2015 Transport properties of pristine few-layer black phosphorus by van der Waals passivation in an inert atmosphere *Nat. Commun.* **6** 6647
- [4] Seyler K L, Schaibley J R, Gong P, Rivera P, Jones A M, Wu S, Yan J, Mandrus D G, Yao W and Xu X 2015 Electrical control of second-harmonic generation in a WSe<sub>2</sub> monolayer transistor *Nat. Nanotechnol.* **10** 407–11
- [5] Yuan H *et al* 2014 Generation and electric control of spin-valley-coupled circular photogalvanic current in WSe<sub>2</sub> *Nat. Nanotechnol.* **9** 851–7
- [6] Rivera P *et al* 2015 Observation of long-lived interlayer excitons in monolayer MoSe<sub>2</sub>–WSe<sub>2</sub> heterostructures *Nat. Commun.* **6** 6242
- [7] Huang C, Wu S, Sanchez A M, Peters J J P, Beanland R, Ross J S, Rivera P, Yao W, Cobden D H and Xu X 2014 Lateral heterojunctions within monolayer MoSe<sub>2</sub>–WSe<sub>2</sub> semiconductors *Nat. Mater.* **13** 1096–101
- [8] Duan X *et al* 2014 Lateral epitaxial growth of two-dimensional layered semiconductor heterojunctions *Nat. Nanotechnol.* **9** 1024–30
- [9] Cheng R, Li D, Zhou H, Wang C, Yin A, Jiang S, Liu Y, Chen Y, Huang Y and Duan X 2014 Electroluminescence and photocurrent generation from atomically sharp WSe<sub>2</sub>/MoS<sub>2</sub> heterojunction p–n diodes *Nano Lett.* **14** 5590–7
- [10] Wang J I J, Yang Y, Chen Y-A, Watanabe K, Taniguchi T, Churchill H O H and Jarillo-Herrero P 2015 Electronic transport of encapsulated graphene and WSe<sub>2</sub> devices fabricated by pick-up of prepatterned hBN *Nano Lett.* **15** 1898–903
- [11] Zhang W, Chiu M-H, Chen C-H, Chen W, Li L-J and Wee A T S 2014 Role of metal contacts in high-performance phototransistors based on WSe<sub>2</sub> monolayers *ACS Nano* **8** 8653–61
- [12] Pradhan N R, Garcia C, Holleman J, Rhodes D, Parker C, Talapatra S, Terrones M, Balicas L and McGill A S 2016 Photoconductivity of few-layered p-WSe<sub>2</sub> phototransistors via multi-terminal measurements *2D Mater.* **3** 041004
- [13] Pradhan N R, Ludwig J, Lu Z, Rhodes D, Bishop M M, Thirunavukkuarasu K, McGill S A, Smirnov D and Balicas L 2015 High photoresponsivity and short photoresponse times in few-layered WSe<sub>2</sub> transistors *ACS Appl. Mater. Interfaces* **7** 12080–8
- [14] Pradhan N R *et al* 2015 Hall and field-effect mobilities in few layered p-WSe<sub>2</sub> field-effect transistors *Sci. Rep.* **5** 8979
- [15] Yamamoto M, Ueno K and Tsukagoshi K 2018 Pronounced photogating effect in atomically thin WSe<sub>2</sub> with a self-limiting surface oxide layer *Appl. Phys. Lett.* **112** 181902
- [16] Chuang H-J, Tan X, Ghimire N J, Perera M M, Chamlagain B, Cheng M M-C, Yan J, Mandrus D, Tománek D and Zhou Z 2014 High mobility WSe<sub>2</sub> p- and n-type field-effect transistors contacted by highly doped graphene for low-resistance contacts *Nano Lett.* **14** 3594–601
- [17] Das S and Appenzeller J 2013 WSe<sub>2</sub> field effect transistors with enhanced ambipolar characteristics *Appl. Phys. Lett.* **103** 103501
- [18] Allain A and Kis A 2014 Electron and hole mobilities in single-layer WSe<sub>2</sub> *ACS Nano* **8** 7180–5
- [19] Britnell L *et al* 2013 Strong light–matter interactions in heterostructures of atomically thin films *Science* **340** 1311–4
- [20] Lopez-Sanchez O, Lembke D, Kayci M, Radenovic A and Kis A 2013 Ultrasensitive photodetectors based on monolayer MoS<sub>2</sub> *Nat. Nanotechnol.* **8** 497–501
- [21] Konstantatos G, Badioli M, Gaudreau L, Osmond J, Bernechea M, de Arquer F P G, Gatti F and Koppens F H L 2012 Hybrid graphene-quantum dot phototransistors with ultrahigh gain *Nat. Nanotechnol.* **7** 363–8
- [22] Terrones H *et al* 2014 New first order Raman-active modes in few layered transition metal dichalcogenides *Sci. Rep.* **4** 4215
- [23] Pradhan N R, Rhodes D, Feng S, Xin Y, Memaran S, Moon B-H, Terrones H, Terrones M and Balicas L 2014 Field-effect transistors based on few-layered  $\alpha$ -MoTe<sub>2</sub> *ACS Nano* **8** 5911–20
- [24] Island J O, Blanter S I, Buscema M, van der Zant H S J and Castellanos-Gomez A 2015 Gate controlled photocurrent generation mechanisms in high-gain In<sub>2</sub>Se<sub>3</sub> phototransistors *Nano Lett.* **15** 7853–8
- [25] Ghosh S, Patil P D, Wasala M, Lei S, Noland A, Sivakumar P, Vajtai R, Ajayan P and Talapatra S 2018 Fast photoresponse and high detectivity in copper indium selenide (CuIn<sub>7</sub>Se<sub>11</sub>) phototransistors *2D Mater.* **5** 015001
- [26] Cao B, Shen X, Shang J, Cong C, Yang W, Eginligil M and Yu T 2014 Low temperature photoresponse of monolayer tungsten disulphide *APL Mater.* **2** 116101
- [27] Bube R H 2004 *Photoelectronic Properties of Semiconductors* (Cambridge: Cambridge University Press)
- [28] Buscema M, Island J O, Groenendijk D J, Blanter S I, Steele G A, van der Zant H S J and Castellanos-Gomez A 2015 Photocurrent generation with two-dimensional van der Waals semiconductors *Chem. Soc. Rev.* **44** 3691–718
- [29] Ghosh S *et al* 2015 Ultrafast intrinsic photoresponse and direct evidence of sub-gap states in liquid phase exfoliated MoS<sub>2</sub> thin films *Sci. Rep.* **5** 11272
- [30] Perea-López N *et al* 2013 Photosensor device based on few-layered WS<sub>2</sub> films *Adv. Funct. Mater.* **23** 5511–7
- [31] Zhang W, Huang J-K, Chen C-H, Chang Y-H, Cheng Y-J and Li L-J 2013 High-gain phototransistors based on a CVD MoS<sub>2</sub> monolayer *Adv. Mater.* **25** 3456–61
- [32] Kim H-J, Kim D-H, Jeong C-Y, Lee J-H and Kwon H-I 2017 Determination of interface and bulk trap densities in high-mobility p-type WSe<sub>2</sub> thin-film transistors *IEEE Electron Device Lett.* **38** 481–4
- [33] Roy K, Padmanabhan M, Goswami S, Sai T P, Ramalingam G, Raghavan S and Ghosh A 2013 Graphene-MoS<sub>2</sub> hybrid structures for multifunctional photoresponsive memory devices *Nat. Nanotechnol.* **8** 826–30